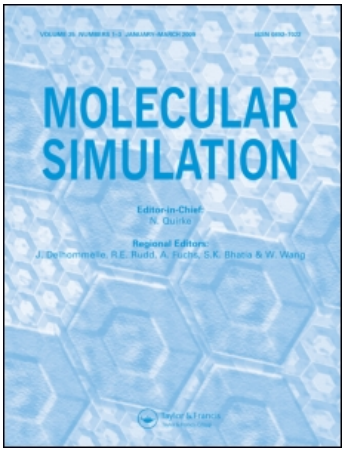

Molecular Simulation
Publication details, including instructions for authors and subscription information:
http://www.informaworld.com/smpp/title~content=t713644482

On the Application of Widom's Test Particle Method to Homogeneous and Inhomogeneous Fluids

Uwe Heinbuch[a]; Johann Fischer[a]
[a] Institut für Thermo- und Fluiddynamik, Ruhr-Universität, Bochum 1, FRG

To cite this Article Heinbuch, Uwe and Fischer, Johann(1987) 'On the Application of Widom's Test Particle Method to Homogeneous and Inhomogeneous Fluids', Molecular Simulation, 1: 1, 109 — 120
To link to this Article: DOI: 10.1080/08927028708080935
URL: http://dx.doi.org/10.1080/08927028708080935

Molecular Simulation, 1987, Vol. 1, pp. 109–120
Photocopying permitted by license only

ON THE APPLICATION OF WIDOM'S TEST PARTICLE METHOD TO HOMOGENEOUS AND INHOMOGENEOUS FLUIDS

UWE HEINBUCH and JOHANN FISCHER*

Institut für Thermo- und Fluiddynamik, Ruhr-Universität, D-4630 Bochum 1, FRG

(*Received May 1987*)

Chemical potentials of a homogeneous and an inhomogeneous Lennard-Jones fluid have been determined by molecular dynamics simulations on the vector computer CYBER 205 by applying essentially the fictitious test particle method of Widom. For the homogeneous fluid we find, contrary to the previous result of Guillot and Guissani, that the simulated chemical potential is independent of the particle number. The crucial point, however, is a sufficiently large cut-off radius in the evaluation of the Boltzmann factor. Comparing with our WCA-type perturbation theory, we get agreement in the chemical potentials within 0.1 kT up to the density $n\sigma^3 = 0.80$ and a difference of 0.2 kT at $n\sigma^3 = 0.85$. For the inhomogeneous case we consider a fluid in a cylindrical pore and integrate Widom's equation over a certain probe volume as suggested earlier by us. Chemical potentials are then calculated independently in five different probe volumes, which are cylindrical shells. The results agree well from the second to the fourth shell. Inaccuracies in the innermost cylinder can be easily explained by bad statistics. In the shell close to the wall the extremely high local density is responsible for the inaccuracies. Extending the probe volume over all cylindrical shells besides the one closest to the wall is thought to yield rather reliable results for the chemical potential. As a by-product of the simulations we also obtained diffusion coefficients, which are given in an appendix.

KEY WORDS: Widom's test particle method, chemical potential, fluids in pores, adsorption, diffusion coefficients.

1. INTRODUCTION

The determination of fluid phase equilibria requires knowledge of entropic thermodynamic quantities, and hence the calculation of the Helmholtz or the Gibbs free energy from computer simulations is of considerable interest. Several methods can be applied for this purpose.

One method is that used in classical thermodynamics, namely integration along an isotherm. Starting from the known Helmholtz energy A of an ideal gas of density n_0 and temperature T, one obtains at density n

$$A(n, T) = A(n_0, T) + \int_{n_0}^{n} pV \frac{dn}{n}. \tag{1}$$

Instead of taking n as the independent variable, one can also take the pressure p and then obtain by a corresponding integration the Gibbs energy G. All subsequent methods can equally well be applied to the canonical as well as to the isobaric–isothermal ensemble. The latter is especially important for mixtures, because their

*To whom correspondence should be sent.

excess properties are usually determined at constant p and T. For convenience, we restrict ourselves here to the canonical ensemble.

A second method is the coupling parameter or charging process, which seems to have been suggested by Kirkwood [1]. In this method one considers a system of particles and changes the total intermolecular potential U by virtue of a parameter λ so that $U = U(\lambda)$. In going from λ_0 to λ_1 the change in the Helmholtz energy is given by

$$A(n, T; \lambda_1) = A(n, T; \lambda_0) + \int_{\lambda_0}^{\lambda_1} \left\langle \frac{\partial U}{\partial \lambda} \right\rangle_\lambda d\lambda, \tag{2}$$

where the angular brackets mean ensemble averaging over $\partial U/\partial\lambda$ which has to be taken at the value λ. The method was first applied by Singer's group for the purpose of calculating excess free energies of mixtures [2, 3]. Currently it is strongly favoured by Haile [4, 5].

Another method is the reweighting procedure suggested by Singer and coworkers [3, 6]. Here, one starts from a reference system with potential energy U_0 and changes the intermolecular interactions to arrive at a potential energy U_1. The corresponding change in the Helmholtz energy is given by

$$A(n, T; \{U_1\}) = A(n, T; \{U_0\}) - kT \ln \langle \exp \{-\beta (U_1 - U_0)\} \rangle_0, \tag{3}$$

where the angular brackets mean ensemble averaging over the reference system. The method works well if the change from U_0 to U_1 is modest. For larger changes, more sophisticated methods like umbrella sampling [7] or marquee sampling [8] have been suggested.

Finally, the test particle method proposed by Widom [9] has to be mentioned. In this method a fictitious test particle is considered that does not influence the "motions" in the simulated system. Let Φ be the potential energy that such a test particle would experience by interacting with all the real particles. Then one measures the average probability of placing the test particle in configuration space. From this one gets the chemical potential μ according to

$$\mu(n, T) = \mu^0(T) + kT \ln n - kT \ln \langle \exp \{-\beta\Phi\} \rangle, \tag{4}$$

where the angular brackets mean ensemble averaging over the simulated system and $\mu^0(T)$ is the temperature dependent part of the ideal gas chemical potential. This method was first applied by Adams [10], and other interesting papers [11–13] followed.

Depending on the system, the above-mentioned methods have certain advantages and disadvantages that have been reviewed elsewhere [14]. The test particle method, especially, has the advantage of not calculating free energy differences; instead it determines an absolute value for the chemical potential. It is, however, believed by some to be restricted to densities that are not too high. Moreover, recently Guillot and Guissani [13] reported the dependence of the chemical potential on the number of real particles in the system.

Our interest was especially in the treatment of strongly inhomogeneous systems, such as fluids in pores. For this purpose the test particle method seems to be most suitable, as it does not require knowledge about a reference system, which is unlikely to be available for such cases. In order to get some experience in implementing the method in a molecular dynamics simulation, we first investigated a homogeneous

Lennard-Jones fluid. Details of that investigation, as well as comparison with previous simulation results and perturbation theory, is given in Section 2. In the following section the inhomogeneous case is covered. Starting from Widom's equation for inhomogeneous fluids [15] we present an integrated form [16] that allows sampling in an arbitrary probe volume in the same way as in the homogeneous case. The method is then applied to a Lennard-Jones fluid in a cylindrical carbon pore. Special attention will be given to the question as to whether the chemical potentials obtained from different probe volumes agree well.

As a by-product of the molecular dynamics simulations we also obtained mean square displacements and diffusion coefficients for the fluid in the pore, which are given in Appendix A.

Finally it should be mentioned that all the calculations were performed with vectorized programs on the vector computer CYBER 205. The methodology of the simulations is given in Appendix B.

2. THE HOMOGENEOUS FLUID

Our motivations for studying the homogeneous fluid was first to see whether the chemical potential calculated by the test particle method really depends on the particle number (as reported recently [13]) and secondly to discover the density up to which this method works reliably.

The methodology of the MD simulations performed for the LJ fluid is given in Appendix B. In the main text we report only those technical details that are crucial to clarify the questions raised above.

It is convenient to use the reduced quantities $\tilde{T} = kT/\varepsilon$ and $\tilde{n} = n\sigma^3$. Lengths will be reduced with respect to σ and then be denoted by a tilde. For the homogeneous case one is interested only in the excess part of the chemical potential defined by

$$\mu^{ex}/kT = -\ln \langle \exp \{-\beta\Phi\} \rangle \tag{5}$$

In their paper [13] Guillot and Guissani investigated an LJ fluid at different densities on the isotherm $\tilde{T} = 1.2$ and varied, at a given state point, the number N of real particles. From their results it seems that the chemical potential depends on N. This dependence becomes stronger with increasing density. It is important, however, to note that their cut-off radius was always half of the cube length a with $\tilde{a} = (N/\tilde{n})^{1/3}$ and hence it also varied with the particle number. In our investigation we introduced two cut-off radii. The one denoted by $r_{c,MD}$ determines the cut-off for the dynamics of the real system and the other represented by $r_{c,BFT}$ determines the cut-off in the determination of the Boltzmann factor of the test particles. Both may be chosen independently, with the exception only that neither may be larger than half the cube length. Our results for the density $\tilde{n} = 0.7$ are displayed in Table 1, which also containes the results of Reference [13] for comparison.

Before we discuss the results in Table 1, it is interesting to report results from two other sources. Powles *et al.* [12] also have calculated the chemical potential with the test particle method for an LJ shifted force system using as cut-off radius $r_c = 3.0$ and 256 particles. Interpolating the raw data for $\tilde{n} = 0.7$ from their Table 1 yields $\mu_1 = -1.574$ for $\tilde{T} = 1.2$. Including their correction $\Delta\mu'$ one obtains finally $\mu^{ex}/kT = -1.95$ for the original LJ system. Moreover, we have also calculated the chemical potential from our WCA-type perturbation theory [17] and obtained $\mu^{ex}/kT = -1.94$.

Table 1 Excess chemical potentials as obtained from the test particle method for an LJ fluid at $\tilde{T} = 1.2$ and $\tilde{n} = 0.7$, using different numbers N of particles and different cut-off radii $r_{c,MD}$ and $r_{c,BFT}$. The radius $r_{c,MD}$ refers to the dynamics of the real particles while the radius $r_{c,BFT}$ refers to the Boltzmann factor of the test particles. The results from Guillot and Guissani (GG) [13] are also included.

N	$\tilde{r}_{c,MD}$	$\tilde{r}_{c,BFT}$	μ^{ex}/kT	$(\mu^{ex}/kT)_{GG}$
108	2.6817	2.6817	−1.68	−1.74
256	2.6817	2.6817	−1.69	
256	3.5756	3.5756	−1.87	−2.00
256	2.6817	3.5756	−1.83	
500	4.4695	4.4695	−1.86	−1.92

Table 2 Excess chemical potentials for an LJ fluid at different high densities as obtained from the test particle method in comparison with perturbation theory (PT) [17] results. (In all cases $r_{c,BFT} = r_{c,MD} = r_c$).

$\tilde{n}$	$\tilde{T}$	N	$\tilde{r}_c$	μ^{ex}/kT	$(\mu^{ex}/kT)_{PT}$
0.7	1.2	500	4.4695	−1.86	−1.94
0.8	1.002	256	3.42	−2.10	−2.20
0.8	2.0	256	3.42	+2.58	+2.49
0.85	1.2	500	4.1894	+0.48	+0.68

Considering our results in Table 1 we learn that going from 108 to 256 particles does not change the chemical potential as long as the cut-off radii $r_{c,MD}$ and $r_{c,BFT}$ are not changed. For 256 particles, however, one gets significantly different results depending on the cut-off radius $r_{c,BFT}$ for the test particle interaction. Increasing the test particle cut-off radius from $\sim 3.5\sigma$ to $\sim 4.5\sigma$ by using 500 particles does not change the result beyond the usual fluctuations. It is nice to see that our simulated chemical potential, for which we take an average value of -1.85, is in reasonable agreement with the perturbation theory result of -1.94. We will return to that point below.

Summarizing, we can say that cutting off the test particle interaction at distances smaller than 3.5σ yields errors in the chemical potential. This may be understood in the following way. If a test particle finds a "hole", i.e. a position with a large value of $\exp\{-\beta\Phi\}$, then the surrounding of that position may not be very uniform and has explicitly to be taken into account up to larger distances.

Our second concern was to clarify the density up to which the method works reliably. For this purpose simulations were made at densities $\tilde{n} = 0.7$, 0.8, and 0.85. It should be mentioned that at the highest density the test particles were inserted into the system after each time step, and hence the number of test particle configurations was 10 times as large there than for the other runs. The results are displayed in Table 2, which contains for comparison also the results of perturbation theory [17], which we believe to work best at high densities. We see that for $\tilde{n} = 0.7$ and for both temperatures at $\tilde{n} = 0.8$ the results from perturbation theory are always lower by about 0.1 kT than those from the test particle method. At $\tilde{n} = 0.85$ the difference, however, is already 0.2 kT and in the opposite direction. As our opinion is that perturbation theory becomes more reliable while the test particle method becomes less reliable with increasing density, we conclude that the test particle method becomes uncertain in the density region between $\tilde{n} = 0.80$ and 0.85.

Summarizing, we can say that the test particle method seems to work up to the

Table 3 Excess chemical potentials for an LJ fluid obtained from the test particle method at low densities in the two-phase region. For $\tilde{n} = 0.2$ comparison with the Haar–Shenker–Kohler (HSK) equation [18] is made; for $\tilde{n} = 0.4$ different particle numbers N have been used. (In all cases $r_{c,BFT} = r_{c,MD} = r_c$).

$\tilde{n}$	$\tilde{T}$	N	$\tilde{r}_c$	μ^{ex}/kT	$(\mu^{ex}/kT)_{HSK}$
0.2	1.2	108	4.0716	−1.31	−1.33
0.4	1.2	108	3.2317	−2.14	
0.4	1.2	256	4.3089	−2.13	
0.4	1.2	500	5.3861	−2.16	

density $\tilde{n} = 0.8$, which is more than 2.5 times the critical density of the Lennard-Jones fluid ($\tilde{n}_c = 0.31$) and only slightly smaller than the triple point density of real argon ($\tilde{n}_t = 0.84$).

As a matter of interest we have also made some simulations at the low densities $\tilde{n} = 0.2$ and 0.4. The results are displayed in Table 3 together with the results of the Haar–Shenker–Kohler (HSK) equation [18] at $\tilde{n} = 0.2$. Despite both densities being in the two-phase region, the chemical potential values obtained with different particle numbers agree remarkably well, and the agreement with the HSK equation is also satisfying.

3. THE INHOMOGENEOUS FLUID

For inhomogeneous fluids a generalization of Eq. (4) is needed. Widom [15] has given that generalization, which is rather similar to Eq. (4), namely

$$\mu = \mu^0 + kT \ln n(\mathbf{r}) - kT \ln \langle \exp\{-\beta\Phi\} \rangle_{\mathbf{r}}. \tag{6}$$

The difference is that the test particle has to be placed at a certain position $\mathbf{r}$ at which the local density $n(\mathbf{r})$ also has to be taken. The potential Φ seen by the test particle is that of the real particles plus that of the external potential. Eq. (6) has already been used by Knight and Monson [19], however, only for a two-dimensional case.

The actual evaluation of Eq. (6) can be made rather similar to the homogeneous case and, as we believe, computationally easier if one introduces an arbitrary probe volume V_p and performs an integration over that volume. This yields

$$\mu = \mu^0 + kT \ln \bar{n} - kT \ln \overline{\langle \exp\{-\beta\Phi\} \rangle}, \tag{7}$$

where the bar means averaging over the probe volume V_p, i.e.

$$\bar{n} = 1/V_p \int n(\mathbf{r})\, d\mathbf{r} = N_p/V_p, \tag{8}$$

and

$$\overline{\langle \exp\{-\beta\Phi\} \rangle} = 1/V_p \int \langle \exp\{-\beta\Phi\} \rangle_{\mathbf{r}} d\mathbf{r}. \tag{9}$$

In order to obtain $\bar{n}$ one simply has to determine the average number N_p of real particles in the probe volume V_p, which can be done more accurately than the determination of the local density $n(\mathbf{r})$. The integration over $\exp\{-\beta\Phi\}$ is performed using an unweighted Monte Carlo procedure. It implies that a certain number M of test particles is thrown at random into the probe volume and their average Boltzmann factor is taken

$$1/V_p \int \langle \exp\{-\beta\Phi\} \rangle_{\mathbf{r}}\, d\mathbf{r} = 1/M \sum \exp\{-\beta\Phi\}. \tag{10}$$

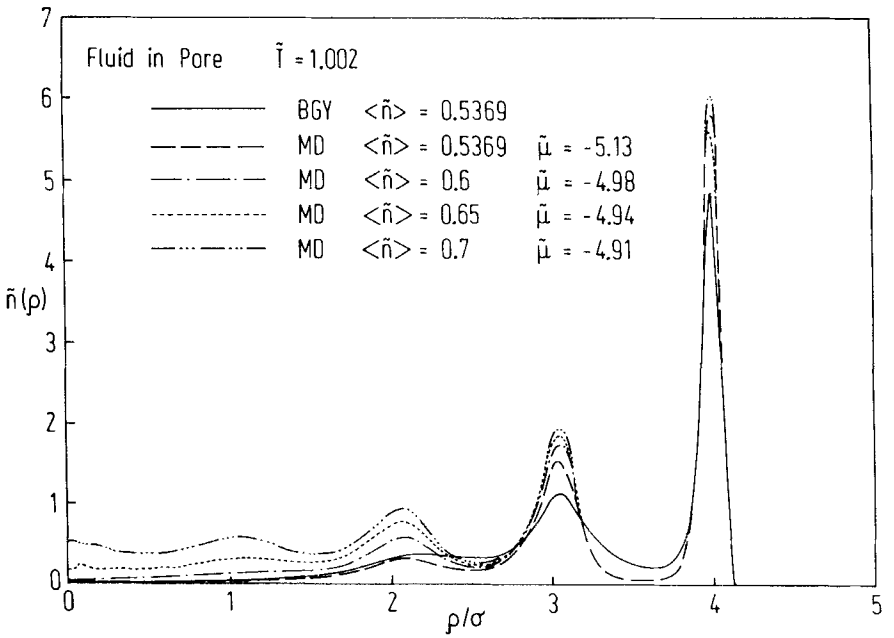

Figure 1 Density profiles of an LJ fluid in a cylindrical carbon pore from molecular dynamics simulations at temperature $\tilde{T} = 1.002$ and different overall densities; the latter refer to a cylinder bounded by the radius 4.5σ. For the lowest density the solution of the Born–Green–Yvon (BGY) equation is also shown. The figure contains the chemical potentials $\tilde{\mu}_{14}$.

Hence, we see that with the integrated form of Widom's equation the procedure for calculating the chemical potential is practically the same as in the homogeneous case. This integrated form has been suggested earlier by us [16] and it is the purpose of this section to present the first results for a three-dimensional system.

The inhomogeneous system we consider is an LJ fluid in a cylindrical pore. The parameters are chosen such that the system corresponds to argon in a carbon pore, which means that the adhesive forces are rather strong. Details of the system and the simulations are given in Appendix B.

The pore considered here has a radius $R_W = 5\sigma$. Runs were made with 366 real particles at $\tilde{T} = 1.002$ and at four different overall densities $\langle\tilde{n}\rangle$, which were adjusted by different heights L of the central cylinder. These parameters are given in Table 4. The resulting density profiles are displayed in Figure 1. We see that the states in the pore essentially differ by the densities in the centre of the pore, which change from gas to liquid densities. For the lowest overall density the solution of the Born–Green–Yvon (BGY) equation in the framework of our approximation scheme [20] is also contained; comparison is made for equal overall density. The agreement between the simulated density profile and that obtained from the BGY equation is reasonable but not so good as in the case of a liquid in a pore [21]. We believe that the discrepancy is partly due to neglecting long-range corrections in the simulations.

Our main concern was to see to what extent the chemical potentials calculated from different probe volumes in the cylinder agree. For this purpose we introduce the radii

Table 4 Chemical potentials of an LJ fluid in a cylindrical pore of radius $R_w = 5\sigma$ at $\tilde{T} = 1.002$. For 366 real particles different overall densities $\langle\tilde{n}\rangle$ were obtained by adjusting the height $\tilde{L}$ of the cylinder; r_c denotes the cut-off radius. The corresponding density profiles are shown in Figure 1. Given are reduced quantities $\tilde{\mu} = (\mu - \mu^0)/kT$. The values $\tilde{\mu}_1$–$\tilde{\mu}_5$ have been obtained from different cylindrical shell probe volumes starting from the axis and ending at the wall. The value $\tilde{\mu}_{14}$ was obtained from a cylinder including the first four shells. In the last column the gas density $\tilde{n}_b$ in a homogeneous fluid at the chemical potential $\tilde{\mu}_{14}$ is given.

$\langle\tilde{n}\rangle$	$\tilde{L}$	$\tilde{r}_c$	$\tilde{\mu}_1$	$\tilde{\mu}_2$	$\tilde{\mu}_3$	$\tilde{\mu}_4$	$\tilde{\mu}_5$	$\tilde{\mu}_{14}$	$\tilde{n}_b$
0.5369	10.17	4.5	−5.09	−5.14	−5.14	−5.12	−5.85	−5.13	0.0063
0.6	9.59	4.5	−5.03	−5.00	−5.00	−4.97	−5.56	−4.98	0.0074
0.65	8.85	4.0	−4.97	−4.93	−4.95	−4.93	−4.93	−4.94	0.0078
0.7	8.22	4.0	−5.04	−4.99	−4.89	−4.89	−4.57	−4.91	0.0080

$\tilde{\varrho}_i = (i - 0.5)$, $i = 1, \ldots, 5$. As first probe volume V_{p1} we take the cylinder with radius $\tilde{\varrho}_1$, the other probe volumes V_{pi} are formed by cylindrical shells between $\tilde{\varrho}_{i-1}$ and $\tilde{\varrho}_i$. After each time step about $(\pi/4) \times 500$ test particles are inserted into all probe volumes. The chemical potentials are then evaluated separately for the probe volumes V_{p1}–V_{p5} and denoted by μ_1–μ_5. At the same time we made a common evaluation for the cylinder containing the volumes V_{p1}–V_{p4}, i.e. for the cylinder bound by $\tilde{\varrho}_4 = 3.5$; this chemical potential is called μ_{14}. The results are given in Table 4.

The chemical potentials μ_2–μ_4 in Table 4 agree quite well. The value μ_1 is somewhat different but still rather close to these results. Its slight scatter can be explained simply by the small probe volume V_{p1} and the resulting bad statistics. Also μ_{14} has the

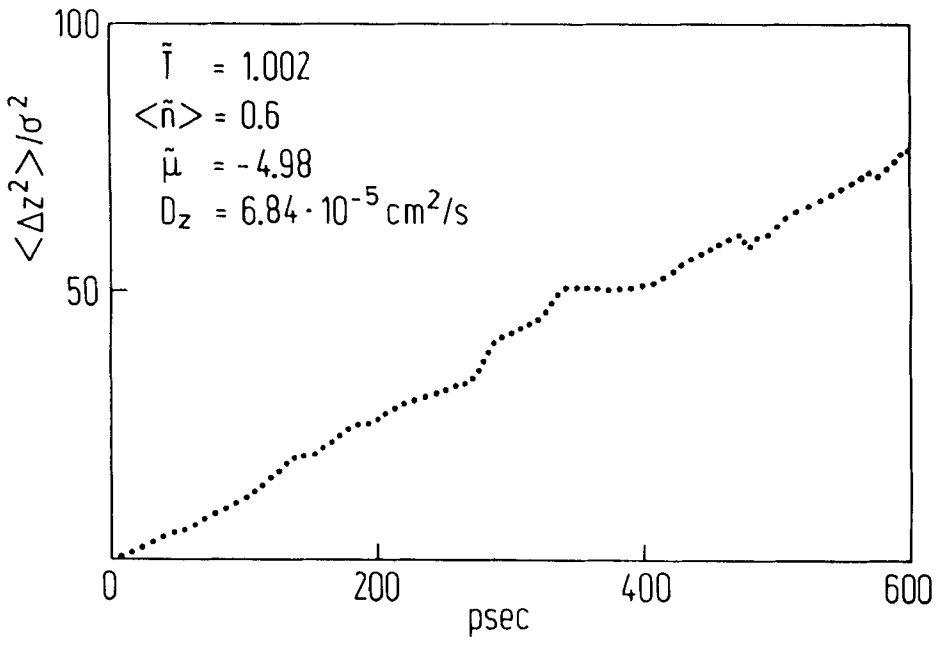

Figure 2 The longitudinal mean square displacement as function of time for an LJ fluid in a cylindrical carbon pore at temperature $\tilde{T} = 1.002$ and overall density $\langle\tilde{n}\rangle = 0.6$. The corresponding density profile is shown in Figure 1.

expected average value between μ_2 and μ_4. The value μ_5, however, differs from the other μ-values considerably except for $\langle\tilde{n}\rangle = 0.65$. The agreement in this case is believed to be a mere coincidence, as for the lower overall densities μ_5 is too small and for the larger density it is too large compared with μ_{14}. The explanation for this difference is thought to be the high density in the layer closest to the wall.

The chemical potential of a fluid in a pore is of interest in determining the state of a homogeneous fluid in equilibrium with the fluid in the pore. Therefore, we have calculated the densities of a homogeneous gas with the same chemical potential. For this purpose the HSK equation [18] was used. The results are also given in Table 4. Note that, from an interpolation [22] between the dew-densities of Adams [23], one obtains at $\tilde{T} = 1.002$ a dew-density $\tilde{n}'' = 0.0264$.

It is also interesting to note that, while the local density in the pore axis changes from a gas- to a liquid-like density with increasing overall density, the chemical potential increases monotonically. That means that we seem to be still above the critical temperature for capillary condensation in that specific pore. One must, however, be a little cautious as the cut-off radius was 4.5σ for the smaller densities, whereas it was only 4.0σ for the larger densities. While the effect of the different cut-off radii will be small on the whole, it could, however, be sufficiently large to create an S-shape in the chemical potentials.

4. SUMMARY

We have found that in applying Widom's test particle method to homogeneous fluids the cut-off radius for the potential seen by the test particle should not be too small. The reason for this is thought to be a non-uniform surrounding of those positions where the test particles can be placed with high probability which dominate the sum over test particle contributions. Moreover, it seems possible to apply the method without difficulties up to densities 2.5 times the critical one.

The method seems to work also for inhomogeneous fluids in a reliable way, if the integrated form is used and the probe volume does not contain regions with very high local densities. We intend to check the present simulation results by comparison with theoretical results to be obtained from approximate chemical potential expressions [24] in connection with our BGY approach.

Acknowledgment

The authors wish to thank Professor J.M. Haile, Clemson, South Carolina, USA, for having introduced them to the molecular dynamics technique. Their cooperation with Professor Haile is supported by NATO travel grant SA.5.2.05 No. RG 471/84.

Die Arbeit wurde mit Unterstützung der Stiftung Volkswagenwerk im Schwerpunkt "Mathematische und Theoretische Grundlagen in den Ingenieurwissenschaften", AZ. I/61 066, durchgeführt.

APPENDIX A: DIFFUSION COEFFICIENTS OF THE FLUID IN THE PORE

As a by-product of the simulations for the fluid in the pore we also obtained mean square displacements and calculated therefrom longitudinal diffusion coefficients.

Table 5 Longitudinal diffusion coefficients D_z for a fluid in a pore. The states are the same as described in Table 4 for which the density profiles are displayed in Figure 1.

$\langle\tilde{n}\rangle$	$D_z[cm^2/s]$
0.5369	7.19×10^{-5}
0.6	6.84×10^{-5}
0.65	5.70×10^{-5}
0.7	5.08×10^{-5}

Such data have been published already by Davis' group [25] and by Suh and MacElroy [26]. Note that our simulations correspond to a gas adsorbed in a cylindrical pore, while in Reference [25] a liquid in a slit pore is considered. The model in Reference [26] considers hard spheres in a hard prism.

For the fluid in the pore with the overall density $\langle\tilde{n}\rangle = 0.6$, the longitudinal mean square displacement as function of time is shown in Figure 2. We note that on the whole $\langle\Delta z^2\rangle$ can be considered to be linear in time. We observe, however, that there are time periods in which $\langle\Delta z^2\rangle$ remains constant or even decreases.

Longitudinal diffusion coefficients D_z were obtained by linear regression analysis of the mean square displacements and the relation

$$\langle\Delta z^2(t)\rangle = 2D_z t. \tag{A1}$$

The results are given in Table 5 for the four fluid states contained in Table 4 and Figure 1. We see that, while the fluid inside the pore is in equilibrium with a homogeneous gas of rather low density, it has a diffusion coefficient typical for a liquid.

Note Added in Proof

The strong deviations of the mean square displacement $\langle\Delta z\rangle^2$ from a straight line seem to be a typical one-dimensional effect. Prof. J.P. Michels (Amsterdam) informed us about similar results obtained from an average of one-dimensional random walks.

APPENDIX B: METHODOLOGY OF THE SIMULATIONS

This appendix sets out the details of the simulations. The molecular dynamics simulations follow closely the primer of Haile [27] using a fifth-order predictor-corrector algorithm due to Gear [28]. The program was vectorized following suggestions of Hoheisel *et al.* [29] using the CYBER 200 FORTRAN language. Test runs were made at constant energy, while in the actual calculations the temperature was kept constant by the momentum scaling procedure [30]. For the following the homogeneous fluid and the fluid in the pore are treated separately.

The Homogeneous Fluid

The Hamiltonian for the real particles consisted of LJ potentials with a cut-off radius $r_{c,MD}$. In different runs different cut-off radii were used; these are given in the main text. Periodic boundary conditions together with the minimum image condition were employed. The initial configuration was that of an fcc lattice and the initial velocities were equal in magnitude but random in orientation. The time steps

were $\Delta t = 0.005\sigma\sqrt{m/\varepsilon}$, i.e. about 10^{-14} s for argon. Equilibration runs were made over 5000 time steps with consecutive production runs over 10 000 time steps.

The potential energy seen by the fictitious test particles was again a sum of LJ potentials with a cut-off radius $r_{c,BFT}$, which could be different from $r_{c,MD}$ and which is given in the main text. Long-range corrections were included putting $g(r) = 1$. Usually after each 10 time steps 500 test particles were inserted at random into the box, which means that for the ensemble averaging 500 000 configurations were evaluated. At the highest density only, $\tilde{n} = 0.85$, the test particles were inserted after each time step, yielding 5 000 000 different configurations.

The Inhomogeneous Fluid

The Hamiltonian consists of the pore potential and of LJ potentials between the fluid particles with a cut-off radius r_c, which was either 4.0σ or 4.5σ and which is given in the main text. No long-range corrections were made.

An infinitely long pore is formed by concentric cylindrical surfaces on which the centres of the solid atoms are smeared out homogeneously [31]. Let R_W be the radius of the innermost cylinder, with further cylinders being placed at $R_W + kd$ ($k = 1, 2, \ldots$). Let us assume that the interaction of one solid atom with one fluid atom at a distance r is given again by a LJ potential $u_{SF}(r)$ and let η be the surface density of the solid atoms on the cylindrical surfaces. The parameters chosen correspond to argon in a carbon pore and are $\varepsilon_{SF}/\varepsilon = 0.4710$, $\sigma_{SF}/\sigma = 1.0035$, $d/\sigma = 0.984$ and $\eta = 4.4266\sigma^{-2}$ with ε and σ being the LJ parameters for the interaction between the fluid particles. The pore potential $u^s(\mathbf{r})$ is the potential from the solid seen by a fluid particle at point $\mathbf{r}$ and obtained by integrating the LJ interaction u_{SF} over the cylinders and summing up the contributions from all cylinders. Note that such a potential corresponds to the $\Sigma 10/4$ potential of Steele [32] for the case of a planar surface. The numerical procedure for calculating $u^s(\mathbf{r})$ for a cylindrical pore is given in Reference [31]. The resulting values depend on the distance ϱ from the pore-axis and are fitted to two polynomial expressions, one of which is used from the pore axis up to some radius ϱ_1 and the other one from ϱ_1 to close to the wall. The minimum of the potential u^s is about -10ε for a pore with $R_W = 5\sigma$.

The initial configuration was constructed by putting monolayers of atoms perpendicular to the cylinder axis. Where the reduced pore radius $\tilde{R}_W$ is an integer, such a monolayer is formed by arranging $3\tilde{R}_W(\tilde{R}_W - 1)$ atoms in a close packed hexagonal two-dimensional lattice around a centre atom situated in the pore axis. The distance between these layers was chosen to give a prescribed overall density $\langle\tilde{n}\rangle$ within the volume bounded by $\varrho_m = R_W - \sigma/2$. The initial velocities were chosen such that for two symmetric particles in a layer the components perpendicular to the axis are equal and the parallel components have equal magnitude but opposite sign. This prescription guarantees that the linear momentum and the angular momentum of the whole fluid parallel to the axis are zero. Note that the perpendicular linear momentum of the whole fluid is not a conserved quantity.

Periodic boundary conditions together with the minimum image convention are used in the direction of the pore axis. The time steps were $\Delta t = 0.002\,\sigma\sqrt{m/\varepsilon}$, which guaranteed a constant total energy and no rise in the temperature [33] over a sufficiently long time in the NVE ensemble (constant particle number N, volume V and energy E). The systems presented were run as NVT ensemble (constant temperature T) over 150 000 production time steps after a period of 50 000 equilibration time steps. The linear and the angular momentum remained sufficiently small over the whole run.

The evaluation of the local density $n(\varrho)$ was made in cylindrical shells with $\Delta\varrho = 0.025\sigma$.

The potential energy seen by the fictitious test particles consisted of the pore potential and a sum of LJ potentials with the real particles cut off at the same distance r_c as was used in the dynamics. No long-range corrections were included. After each time step about $(\pi/4) \times 500$ test particles were thrown into the cylinder with radius ϱ_m.

References

[1] J.G. Kirkwood, "Statistical mechanics of fluid mixtures", *J. Chem. Phys.*, **3**, 300 (1935).

[2] I.R. McDonald, "NpT-ensemble Monte Carlo calculations for binary liquid mixtures", *Molec. Phys.*, **23**, 41 (1972).

[3] J.V.L. Singer and K. Singer, "Monte Carlo calculations of thermodynamic properties of binary mixtures of Lennard-Jones (12-6) liquids", *Molec. Phys.*, **24**, 357 (1972).

[4] J.M. Haile, "On the use of computer simulation to determine the excess free energy in fluid mixtures", *Fluid Phase Equilibria*, **26**, 103 (1986).

[5] M. Bohn, J. Fischer and J.M. Haile, "Effect of molecular elongation on the quadrupolar free energy in diatomic fluids", *Molec. Phys.*, to be submitted.

[6] I.R. McDonald and K. Singer, "Calculation of thermodynamic properties of liquid argon from Lennard-Jones parameters by a Monte Carlo method", *Disc. Faraday Soc.*, **43**, 40 (1967).

[7] G.M. Torrie and J.P. Valleau, "Monte Carlo free energy estimates using non-Boltzmann sampling: application to the sub-critical Lennard-Jones fluid", *Chem. Phys. Lett.*, **28**, 578 (1974).

[8] G. Jacucci and N. Quirke, "Monte Carlo calculation of the free energy difference between hard and soft core diatomic liquids", *Molec. Phys.*, **40**, 1005 (1980).

[9] B. Widom, "Some topics in the theory of fluids", *J. Chem. Phys.*, **39**, 2808 (1963).

[10] D.J. Adams, "Chemical potential of hard-sphere fluids by Monte Carlo methods", *Molec. Phys.*, **28**, 1241 (1974).

[11] S. Romano and K. Singer, "Calculation of the entropy of liquid chlorine and bromine by computer simulation", *Molec. Phys.*, **37**, 1765 (1979).

[12] J.G. Powles, W.A.B. Evans and N. Quirke, "Non-destructive molecular-dynamics simulation of the chemical potential of a fluid", *Molec. Phys.*, **46**, 1347 (1982).

[13] B. Guillot and Y. Guissani, "Investigation of the chemical potential by molecular dynamics simulation", *Molec. Phys.*, **54**, 455 (1985).

[14] K.S. Shing and K.E. Gubbins, "A review of methods for predicting fluid phase equilibria: theory and computer simulation", in *Molecular-Based Study of Fluids*, J.M. Haile and G.A. Mansoori, eds, Advances in Chemistry Series 204, American Chemical Society, Washington, 1983, ch.4. G. Jacucci and N. Quirke, "Free energy calculations for crystals", in *Computer Simulation of Solids*, C.R.A. Catlow and W.C. MacKrodt, Lecture Notes in Physics, Vol. 166, Springer-Verlag, Berlin, 1982.

[15] B. Widom, "Potential distribution theory and the statistical mechanics of fluids", *J. Phys. Chem.*, **86**, 869 (1982).

[16] U. Heinbuch and J. Fischer, "Model studies of adsorption on plane interfaces and in pores", in *Proc. Sec. Conf. Fundamentals of Adsorption Santa Barbara 1986*, A.I. Liapis, ed., Engineering Foundation AIChE, NY, 1987, p. 245.

[17] J. Fischer, "Perturbation theory for the free energy of two-center-Lennard-Jones liquids", *J. Chem. Phys.*, **72**, 5371 (1980).

[18] J. Fischer and M. Bohn, "The Haar–Shenker–Kohler equation: a fundamental equation of state", *Molec. Phys.*, **58**, 395 (1986).

[19] J.F. Knight and P.A. Monson, "Computer simulation of adsorption equilibrium for a gas on a solid surface using the potential distribution theory", *J. Chem. Phys.*, **84**, 1909 (1986).

[20] J. Fischer and M. Methfessel, "Born–Green–Yvon approach to the local densities of a fluid at interfaces", *Phys. Rev. A*, **22**, 2836 (1980).

[21] U. Heinbuch and J. Fischer, "Liquid argon in a cylindrical carbon pore: molecular dynamics and Born–Green–Yvon results", *Chem. Phys. Letters*, **135**, 587 (1987).

[22] J. Fischer, U. Heinbuch and M. Wendland, "On the hard sphere plus attractive mean field approximation for inhomogeneous fluids", *Molec. Phys.*, **60**, in press.

[23] D.J. Adams, "Calculating the low temperature vapour line by Monte Carlo", *Molec. Phys.*, **32**, 647 (1976).

[24] J. Fischer and U. Heinbuch, "Relationship between free energy density functionals and Born–Green–Yvon approaches for inhomogeneous fluids", *J. Chem. Phys.*, submitted.
[25] J.J. Magda, M. Tirrell and H.T. Davis, "Molecular dynamics of narrow, liquid-filled pores", *J. Chem. Phys.*, **83**, 1888 (1985).
[26] S.H. Suh and J.M.D. MacElroy, "Molecular dynamics simulation of hindered diffusion in micro-capillaries", *Molec. Phys.*, **58**, 445 (1986).
[27] J.M. Haile, "A primer for molecular dynamics simulations", private communication.
[28] C.W. Gear, *Numerical Initial Value Problems in Ordinary Differential Equations*, Prentice-Hall, Englewood Cliffs, 1971.
[29] R. Vogelsang, M. Schoen and C. Hoheisel, "Vectorization of molecular dynamics Fortran programs using the CYBER 205 vector processing computer", *Computer Physics Communication*, **30**, 235 (1983).
[30] J.M. Haile and S. Gupta, "Extensions of the molecular dynamics simulation method. II. Isothermal systems", *J. Chem. Phys.*, **79**, 3067 (1983).
[31] J. Fischer, M. Bohn, B. Körner and G.H. Findenegg, "Supercritical gas adsorption in porous materials. II. Prediction of adsorption isotherms", *German Chem. Eng.*, **6**, 84 (1983).
[32] W.A. Steele, *The Interaction of Gases with Solid Surfaces*, Pergamon Press, Oxford, 1974.
[33] D. Fincham, "Choice of timestep in molecular dynamics simulation", *Computer Physics Communications*, **40**, 263 (1986).